Agricultural Water Management 132 (2014) 37–45

Contents lists available at ScienceDirect

Agricultural Water Management

journal homepage: www.elsevier.com/locate/agwat

Drought monitoring using a Soil Wetness Deficit Index (SWDI) derived from MODIS satellite data

Mohammad Reza Keshavarz[a,*], Majid Vazifedoust[b], Amin Alizadeh[a]

[a] College of Agriculture, Ferdowsi University of Mashhad, Iran
[b] College of Agriculture, Guilan University, Guilan, Iran

ARTICLE INFO

Article history:
Received 26 April 2013
Accepted 10 October 2013

Keywords:
Drought
Soil wetness
SWDI
Remote sensing

ABSTRACT

Soil moisture is considered a key index of agricultural drought monitoring systems due to its importance for plant growth and biological interactions. In this research, a Soil Wetness Deficit Index (SWDI) was developed based on a Soil Wetness Index to evaluate soil moisture deviation as an indicator of agricultural drought. The Soil Wetness Index is derived using a triangle space concept between the land surface temperature (LST) and vegetation index (NDVI). To acquire the triangle space concept, 8-day-products of land surface reflectance and LST derived from MODIS satellite data over Isfahan were used. The data was collected in the period of 2000–01 (dry year) and 2004–05 (wet year) on an 8-day time step. The results indicated that the SWDI index has the capability of mapping the spatial distribution of areas affected by drought, as well as the drought intensity. The estimated cumulative number of dry days (with $-4 < SWDI < 0$) in the period of 2000–01 was 184 days. The results also confirmed the existence of wet days in the period 2004–05. Moreover, shifts in drought condition at the end of the wet and dry periods were detected in the area. Results also showed that the presence of vegetation plays an important role in balancing soil moisture variation.

1. Introduction

Drought is the result of climate variations that infrequently occur in vast geographic areas without any specific border. Drought affects food security more than any other natural disaster. Predicting when a drought will occur and the length of its duration is very difficult compared to other disasters such as flood flashing (Kogan, 1997). Based on the environmental sub-system it affects, droughts are classified into meteorological, soil moisture (agricultural), hydrological and famine (Peters, 2003).

Soil moisture content plays an effective role in agricultural drought (Kuenzer et al., 2008). Root zone moisture content is commonly assigned to the upper 1–2 m of soil profile. This moisture is generally available for crop growth and can be transported to the atmosphere through the evapo-transpiration process (Verstraeten, 2006). Considering the effect of soil moisture on plant growth and crop productions, estimating soil moisture content is very important in monitoring agricultural drought. Nonetheless, due to the extreme variation of soil moisture along a day, it cannot be an appropriate index of drought severity by itself. Hence, an index is needed to consider the long-term variation of the soil moisture. Also, the index should be able to compare the soil moisture deficit across seasons.

Principally, soil moisture monitoring using field scale methods is very expensive, time consuming and impossible for application in vast areas. Additionally, converting field scale soil moisture data to geo-spatial maps using geo-statistical methods have no adequate quality. Therefore, there is a need for special tools that monitor spatial and temporal soil moisture variations continuously and accurately. Due to higher spatial and temporal resolution, methods based on remote sensing techniques in contrast to field measurements and simulation models are preferred for the regional purposes.

Over the past two decades, numerous approaches have been developed for regional estimation of soil moisture. Some of these have been based on remotely sensed optical and microwave data. Methods include the use reflective data (Peters et al., 1991; Wang et al., 2007), thermal infrared data (Crow et al., 2008; Gillies and Carlson, 1995; Qui, 2006), passive and active microwave data (De Ridder, 2000; Mattia et al., 2008; Moran et al., 2004). Due to higher scatter in interaction with aerosols and lower penetration into the surface, optical and thermal imagery is more limited in comparison to radar and microwave imagery. However, because of high spatial and temporal resolution and high correlation between soil moisture and surface temperature, implementation of optical and thermal imagery methods has increased in the recent years (Verstraeten, 2006).

* Corresponding author. Tel.: +98 9126514204.
E-mail address: mohammadreza.4231@gmail.com (M.R. Keshavarz).

0378-3774/$ – see front matter © 2013 Elsevier B.V. All rights reserved.
http://dx.doi.org/10.1016/j.agwat.2013.10.004

Table 1
Characteristic of satellite data used for computing Soil Wetness Index.

Satellite	Sensor	Spatial resolution (m)	Temporal resolution (day)	Selected products	Acquisition dates
Terra	MODIS	250	8	MOD09Q1	2000–2001 from September to July and 2004–2005 from September to July
		1000 (resample to 250 m)	8	MOD11A2	
TRMM		25,000 (resample to 250 m)	8	3B42RT	2000–2001 from September to July and 2004–2005 from September to July

Plants are sensitive to water stress and the amount of stress can be detected using vegetation indices derived from optical satellite data (Marshall, 2005). Vegetation indices derived from spectral reflection are the most common techniques for estimating physical characteristics of crops such as moisture content in the leaves and pigment concentration (Cheng et al., 2008; Gao, 1996; Huete et al., 1997; Peñuelas et al., 1997; Ustin et al., 2004).

For instance, NDVI (Normalized Difference Vegetation Index) is a well known vegetation index which shows a promising correlation with short term variation of soil moisture (Peters et al., 1991; Wang et al., 2007). NDVI can be obtained using surface reflection in the visible and near infrared sections of electromagnetic (EM) spectrum. Adegoke and Carleton (2002), and Wang et al. (2007) studied direct relation between soil moisture and NDVI, and confirmed the delay effect of soil moisture on NDVI. Wang et al. (2007) also showed that the relationship between NDVI and soil moisture is more reliable with less delay in the semi-arid regions. Although, land surface temperature (LST) is also dependent on soil moisture and fractional vegetation cover, no universal and direct relation between LST and soil moisture has been reported (Mallick et al., 2009). However, due to an increase of LST over areas with low NDVI in the arid region, a negative relation between LST and NDVI is expected. In many studies, a triangular (or trapezoidal) space concept method that is defined as a physical relationship between NDVI and LST in the form of scatter plots, has been recommended for average soil moisture in the root zone (Carlson, 2007; Keshavarz et al., 2011; Mallick et al., 2009; Stisen et al., 2008; Wang et al., 2006;).

In this research, a Soil Wetness Deficit Index (SWDI) was developed based on Soil Wetness Index (SWI) derived from applying a triangle space concept between LST and NDVI to evaluate soil moisture deviation as an indicator of agricultural drought.

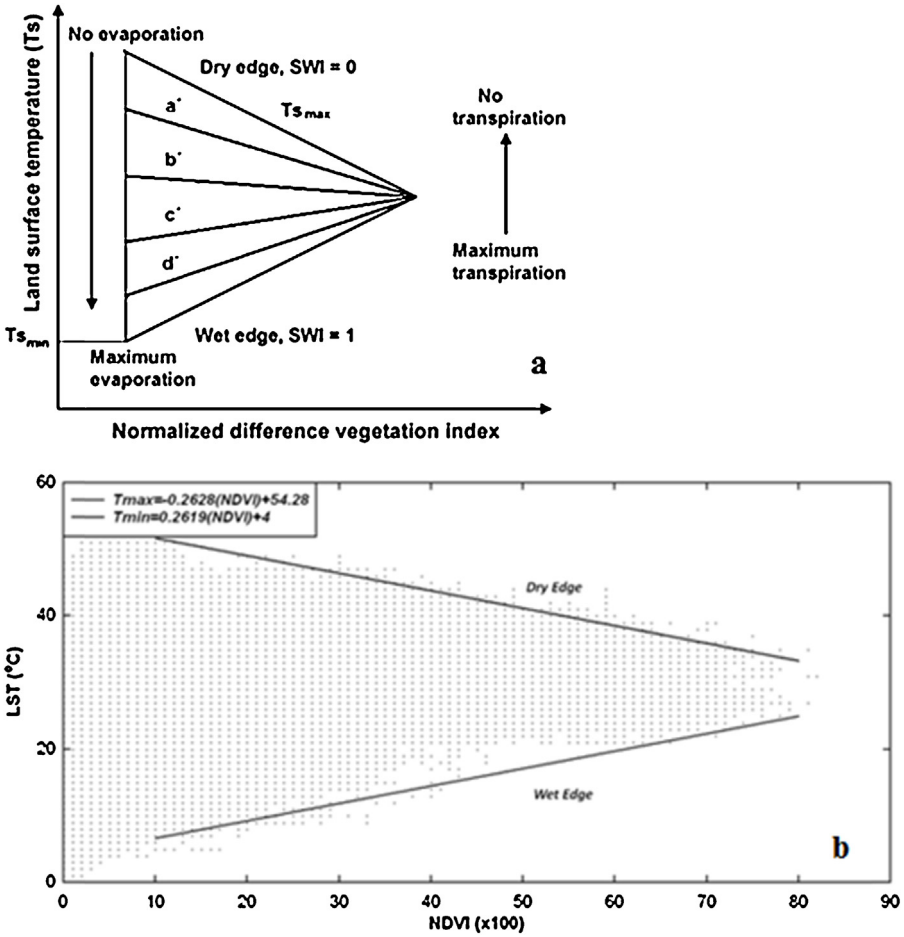

Fig. 1. (a) Conceptual diagram of LST–NDVI triangle for determining Soil Wetness Index. The value of SWI is zero along the dry edge and its value is 1 along the wet edge. The intermediate SWI isolines at 0.2, 0.4, 0.6 and 0.8 are represented by a′, b′, c′ and d′, respectively (Mallick et al., 2009). (b) A sample of triangular variant between Land Surface Temperature and Normalized Difference Vegetation Index over Isfahan on a clear day (DOY 105: 15 April 2005).

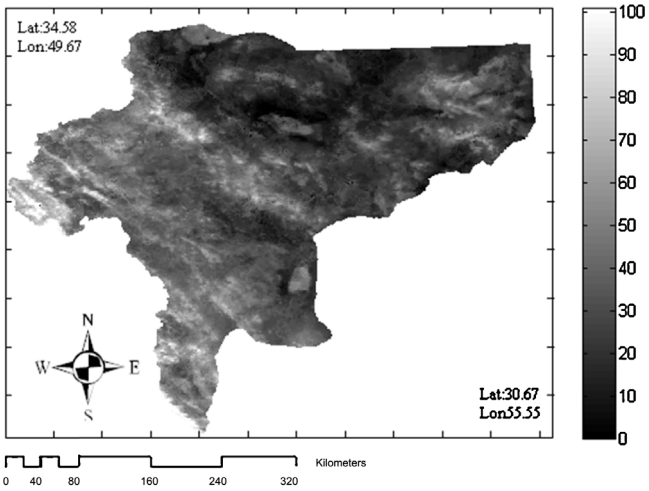

Fig. 2. A sample of spatial distribution of Soil Wetness Index (%) over Isfahan on a clear day (DOY 81: 22 March 2001).

2. Materials and methods

2.1. Study area

The study area (Isfahan province) is located in the central parts of Iran and has an area of 214,503 km^2. It covers an area from 30.6N to 34.58N and from 49.6E to 55.5E. The area has a semi-arid climate with a limited amount of precipitation (130 mm per year which generally occurs in winter from December to April). About 3% of total area is cultivated (609,250 ha) from which 95% is assigned to the irrigated lands and 5% is assigned to rain-fed lands. The maximum temperature is 30 °C in July and the minimum temperature is 3 °C in January (Akbari et al., 2007).

2.2. Data preparation and image processing

Short-term variation of surface soil moisture in the vegetated landscapes with greater spatial details can be monitored through optical–thermal infrared band data from moderate resolution (250 m–1 km) sensors (e.g. MODIS TERRA and AQUA) having two overpasses per day (Mallick et al., 2009). MODIS products of LSR (MOD09Q1) and LST (MOD11A2) with 250 and 1000 m spatial resolutions implemented for the periods of September 2000–July 2001 and September 2004–July 2005 over Isfahan (tile h22v05) were utilized. NDVI was produced using satellite data from channel one (~660 nm) and channel two (~860 nm) that cover visible and near infrared part of EM spectrum. The data was geometrically corrected and its projection system was converted from sinusoidal to UTM.

In addition, satellite data of rainfall from the Tropical Rainfall Measuring Mission (TRMM) was compared with SWI. TRMM, a cooperative effort between NASDA of Japan and NASA of the USA, has been designed to measure rain rates from space using a consortium of sensors including: high resolution radar, passive microwave radiometer and visible-infrared radiometer. For the purposes of this research, cumulative rainfall data was retrieved from TRMM product (3B42RT) for each dry and wet period. To overlay the TRMM data on other spatial data (i.e. NDVI, SWI maps), the images were reassembled into 250 m spatial resolutions using a nearest neighborhood method. The remaining image processing was performed using an automated program developed in MATLAB. Table 1 shows the main characteristics of the satellite data utilized in this study.

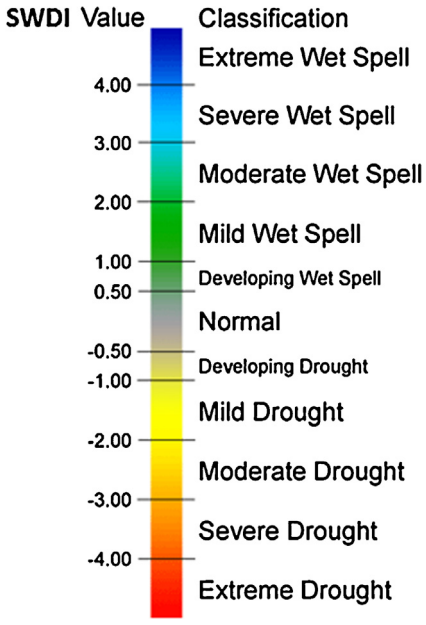

Fig. 3. SWDI value classification.

Table 2
Comparison of global mean of SWI, NDVI and LST in the periods of 2000–01 and 2004–05 over study area (positive sign indicates existence of a significant difference in specified level of probability) using Duncan method in under irrigation farms.

	Level		Mean value		Error freedom Degree	CV
	0.05	0.01	2000–01	2004–05		
LST (°C)	+	+	23.43	21.76	36	23
SWI	+	+	42%	44%	36	11.67
NDVI	+	+	0.166	0.179	36	8

2.3. Soil Wetness Index (SWI)

To extract soil moisture, a triangular space concept between LST and NDVI data was implemented. As shown in Fig. 1a, the highest LST along the dry edge represents the driest soil condition when the soil wetness is near zero. The wettest (near saturated) soil conditions are represented through the minimum LST along the wet edge when the surface soil wetness is greatest. It is assumed that moisture availability varies linearly from the dry edge to the wet edge. An example of the concept is shown in Fig. 1b. The figure shows a scatter plot of NDVI versus LST in a specific time step and wet and dry edges are shown clearly. With this assumption, Soil Wetness Index (SWI) can be computed for each pixel by the following equation (Mallick et al., 2009):

$$\mathrm{SWI}_i = \frac{T_{\max(i)} - T_{s(i)}}{T_{\max(i)} - T_{\min(i)}} \quad (1)$$

where i indicates pixel number, $T_{s(i)}$ is the LST for ith pixel, $T_{\min(i)}$ and $T_{\max(i)}$ are minimum and maximum values of observed LST

Table 3
Comparison of global mean of SWI, NDVI and LST in the periods of 2000–01 and 2004–05 over study area (positive sign indicates existence of a significant difference in specified level of probability) using Duncan method in dry farms.

	Level		Mean value		Error freedom Degree	CV
	0.05	0.01	2000–01	2004–05		
LST (°C)	+	+	36.03	27.41	36	6.8
SWI	+	+	55%	64%	36	11.71
NDVI	–	–	0.134	0.13	36	13.89

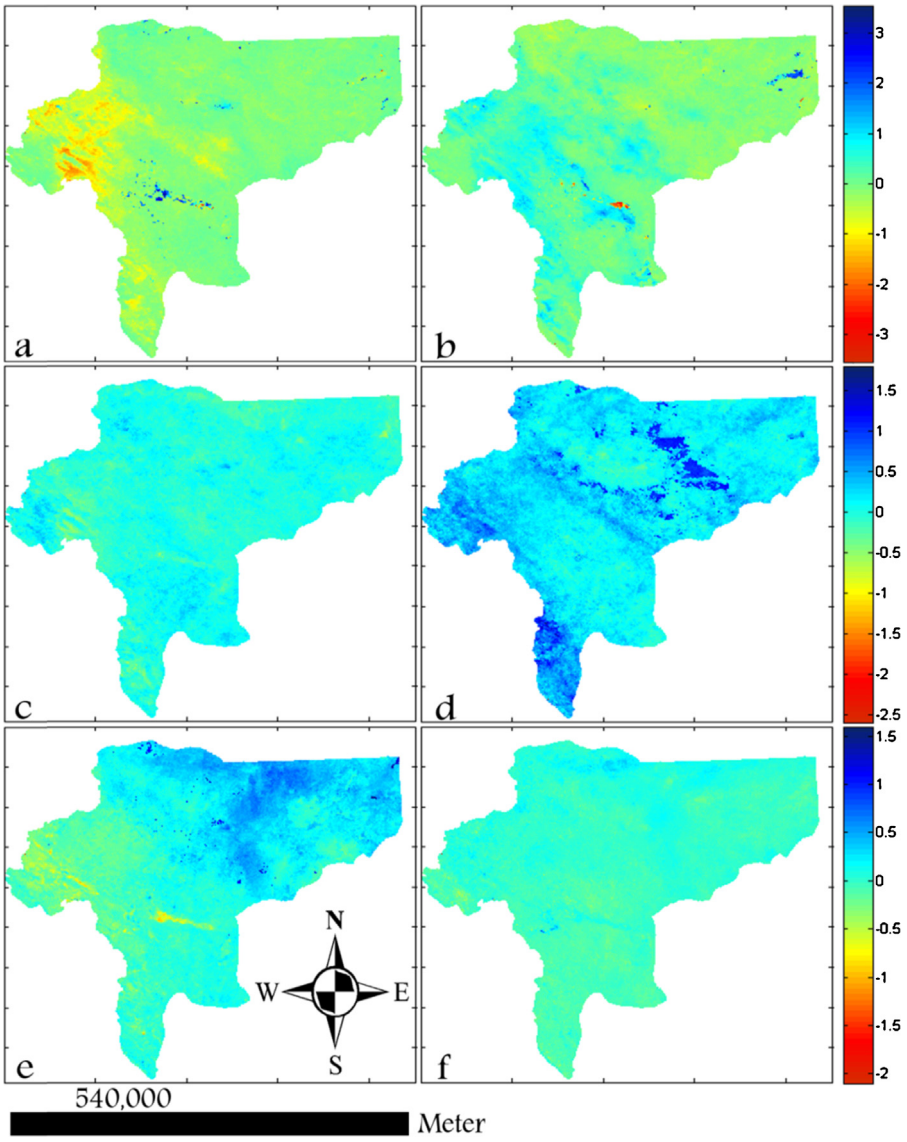

Fig. 4. Spatial distribution of SWDI in over Isfahan province in two periods and three time section ((a) 2001: 017, (b) 2005: 017, (c) 2001: 073, (d) 2005: 073, (e) 2001: 183, (f) 2005: 183).

for the *i*th NDVI. T_{min} and T_{max} are derived using linear relations between NDVI and LST on the dry and wet edges as below:

$$T_{max(i)} = b + a(\mathrm{NDVI}_{(i)}) \quad (2)$$

$$T_{min(i)} = d + c(\mathrm{NDVI}_{(i)}) \quad (3)$$

where *a*, *b*, *c* and *d* are slope and offset values of diagonal lines on the dry and wet edges respectively. A spatial distribution of SWI is represented in Fig. 2.

2.4. Developing a drought index

To evaluate soil moisture variations in the dry and wet periods, a Soil Wetness Deficit Index (SWDI), was developed based on SWI values with 8-day time steps as:

$$\mathrm{SD}_i = \frac{\mathrm{SWI}_i - \mathrm{MSWI}_j}{\max \mathrm{SWI} - \min \mathrm{SWI}} \times 100 \quad (4)$$

where, SD_i is soil moisture deficit in the *i*th 8-day-period, MSWI_j is long term mean of observed SWI in the *j*th month, max SWI (=100%) and min SWI (=0%) are maximum and minimum possible values for SWI.

By using Eq. (4) the seasonality inherent in soil water was removed. Hence, the deficit values can be compared across seasons. The SD values during an 8-day period range from −100 to +100 indicating very dry to very wet conditions. Drought occurs only when the dryness continues for a prolonged period of time which can affect crop growth. As the limits of SD values were between −100 and +100, the worst drought can be represented by a straight line with the following equation:

$$\sum_{t=1}^{i} \mathrm{SD}_t = -100t - 100 \quad (5)$$

where, *t* represents the number for each 8-day-period of *i* consecutive 8-day-periods with negative SD (See *Z* index in Palmer, 1965 for more details). SWDI, for any given time step can be calculated by:

$$\mathrm{SWDI}_i = \frac{\sum_{t=1}^{i} \mathrm{SD}_t}{25t + 25} \quad (6)$$

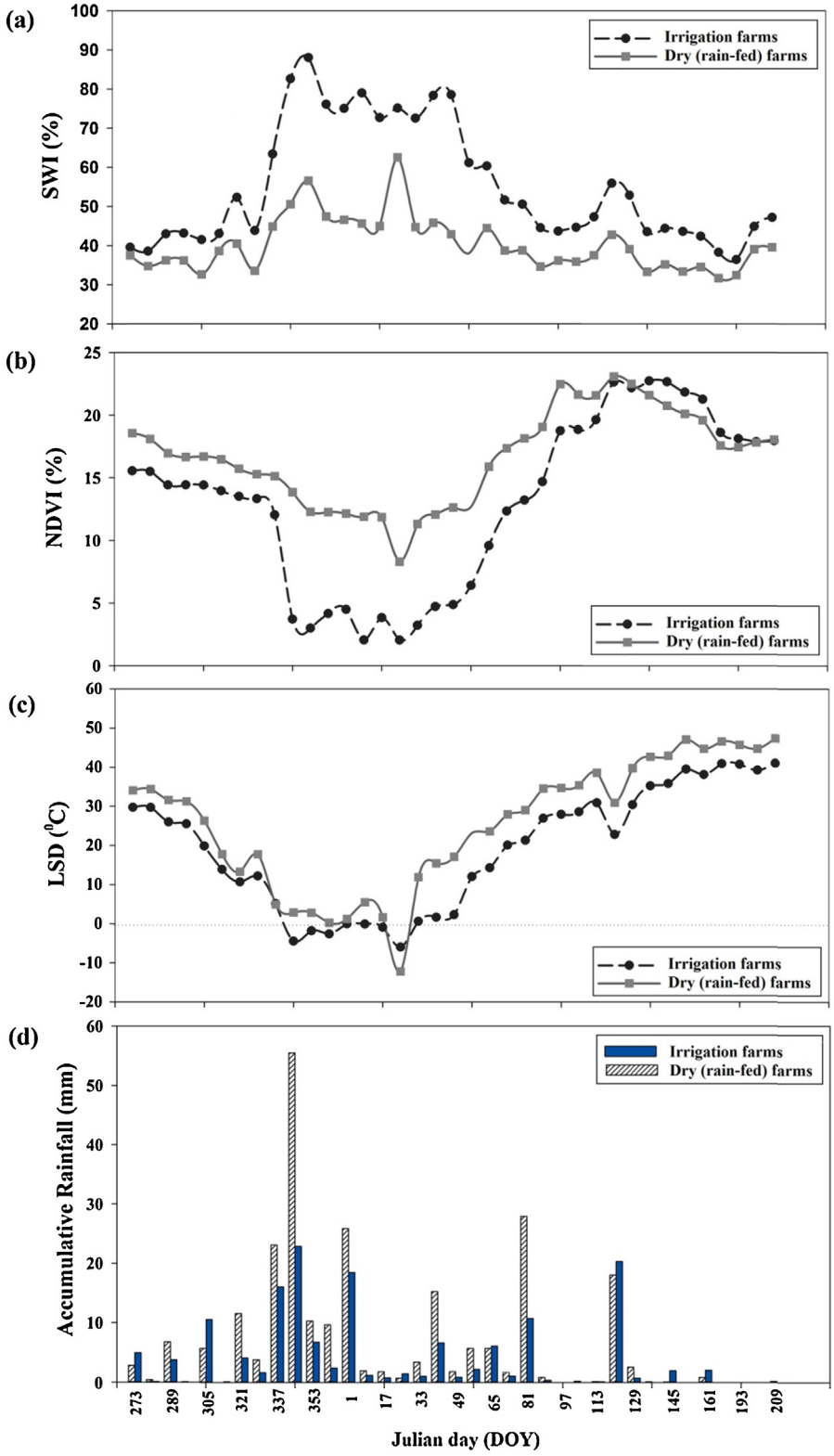

Fig. 5. (a) Global mean of SWI (%) variation of dry (rain-fed) farms and under irrigation farms in the dry period (2000–01). (b) Global mean of NDVI (%) variation of dry (rain-fed) farms and under irrigation farms in the dry period (2000–01). (c) Global mean of LST (°C) variation of dry (rain-fed) farms and under irrigation farms in the dry period (2000–01). (d) Global mean of 8-day accumulative rainfall (mm) of dry (rain-fed) farms and under irrigation farms. Horizontal axes represents Julian day (starts from DOY 273 of 2000 and ends in DOY 209 of 2001).

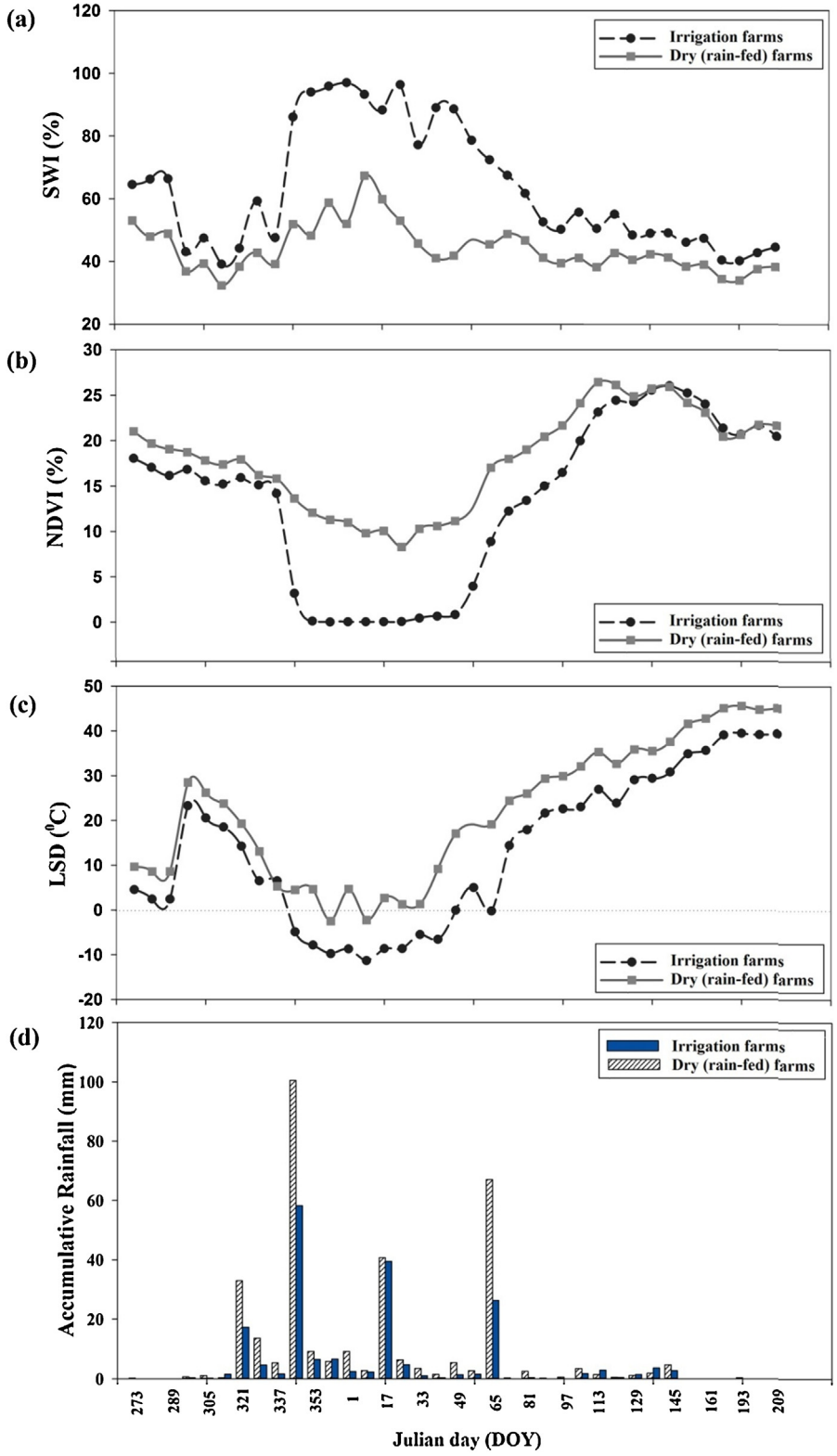

Fig. 6. (a) Global mean of SWI (%) variation of dry (rain-fed) farms and under irrigation farms in the wet period (2004–05). (b) Global mean of NDVI (%) variation of dry (rain-fed) farms and under irrigation farms in the wet period (2004–05). (c) Global mean of LST (°C) variation of dry (rain-fed) farms and under irrigation farms in the wet period (2004–05). (d) Global mean of 8-day accumulative rainfall (mm) of dry (rain-fed) farms and under irrigation farms. Horizontal axes represents Julian day (starts from DOY 273 of 2004 and ends in DOY 209 of 2005).

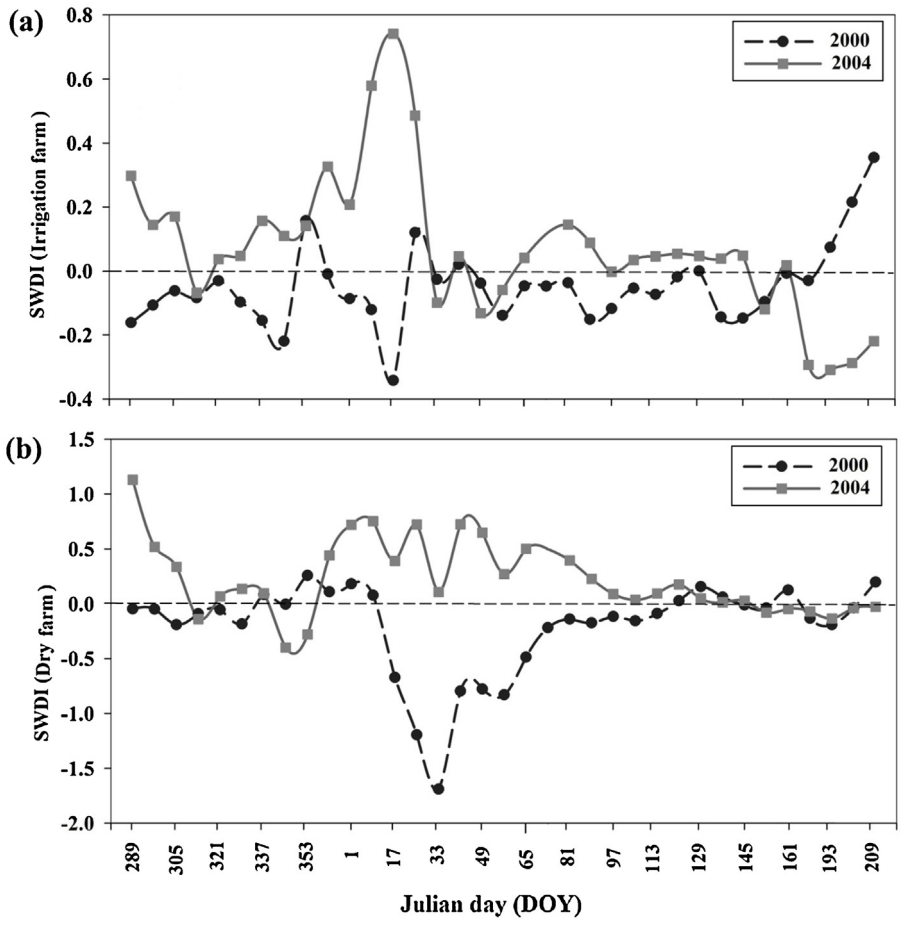

Fig. 7. (a) SWDI variation of an under irrigation farm (Lat: 32°48′ Lon: 51°38′) in two periods of time. (b) SWDI variation of a Dry farm (Lat: 31°14′ Lon: 51°00′) in two periods of time. Horizontal axes represents Julian day (starts from DOY 273 of 2000 or 2004 and ends in DOY 209 of the next year).

To determine drought severity, the main challenge is to choose the time step over which the dryness values need to be accumulated. In order to overcome this problem the drought index was calculated on an incremental basis (Eq. (7)) as suggested by Palmer (1965) and Narasimhan and Srinivasan (2005):

$$\mathrm{SWDI}_i = \mathrm{SWDI}_{i-1} + \Delta\mathrm{SWDI}_i \tag{7}$$

In order to evaluate the contribution to drought severity of each 8-day-period, set $i = 1$ and $t = 1$ in Eq. (6):

$$\mathrm{SWDI}_1 = \frac{\mathrm{SD}_1}{50} \tag{8}$$

Then,

$$\mathrm{SWDI}_1 - \mathrm{SWDI}_0 = \Delta\mathrm{SWDI}_1 = \frac{\mathrm{SD}_1}{50} \tag{9}$$

A drought will not continue in the extreme category if subsequent months are normal or near normal ($-1 < \mathrm{SWDI} < 1$). Therefore, the rate at which SD must increase in order to maintain a constant value of SWDI depends on the value of SWDI to be maintained. For this reason, an additional term must be added to Eq. (9) for all months following an initial dry month:

$$\Delta\mathrm{SWDI}_i = \frac{\mathrm{SD}_i}{50} + c \cdot \mathrm{SWDI}_{i-1} \tag{10}$$

By assuming SWDI is −4 during subsequent time steps, SD_i should be −100:

$$\Delta\mathrm{SWDI}_i = \frac{-100}{50} + c(-4.0),$$

$$0 = -2 - 4c,$$

$$c = -0.5$$

Therefore, drought severity in any given time step is given by:

$$\mathrm{SWDI}_i = \mathrm{SWDI}_{i-1} + \frac{\mathrm{SD}_i}{50} - 0.5\,\mathrm{SWDI}_{i-1}$$

$$\mathrm{SWDI}_i = \frac{\mathrm{SD}_i}{50} + 0.5\ \mathrm{SWDI}_{i-1} \tag{11}$$

SWDI ranges from −4 to +4, representing dry to wet conditions (Fig. 3).

3. Results and discussion

The SWI values in 8-day steps were derived from satellite data using LST and NDVI maps and an automated program written in MATLAB.

Fig. 4 shows spatial distribution of the SWDI index at three different time periods (DOY: 17, 73 and 185) in 2001 and 2005. Fig. 4a and b represents SWDI for DOY 17 in 2001 and 2005, respectively. Each 8-day time step is referred to the first day of the period. For example, SWDI of DOY 17 represents mean value of SWDI of DOY 17–DOY 24. As shown in this figure, SWDI values vary from −2 to 0 in 2001: 17 (Fig. 4a) and approximately the entire area (almost 85%) is subjected to drought ($\mathrm{SWDI} < 0$). The only part which is experiencing a wet spell is located in the central parts represented by the pixels around the main river (Zayanderoud). Fig. 4b shows the

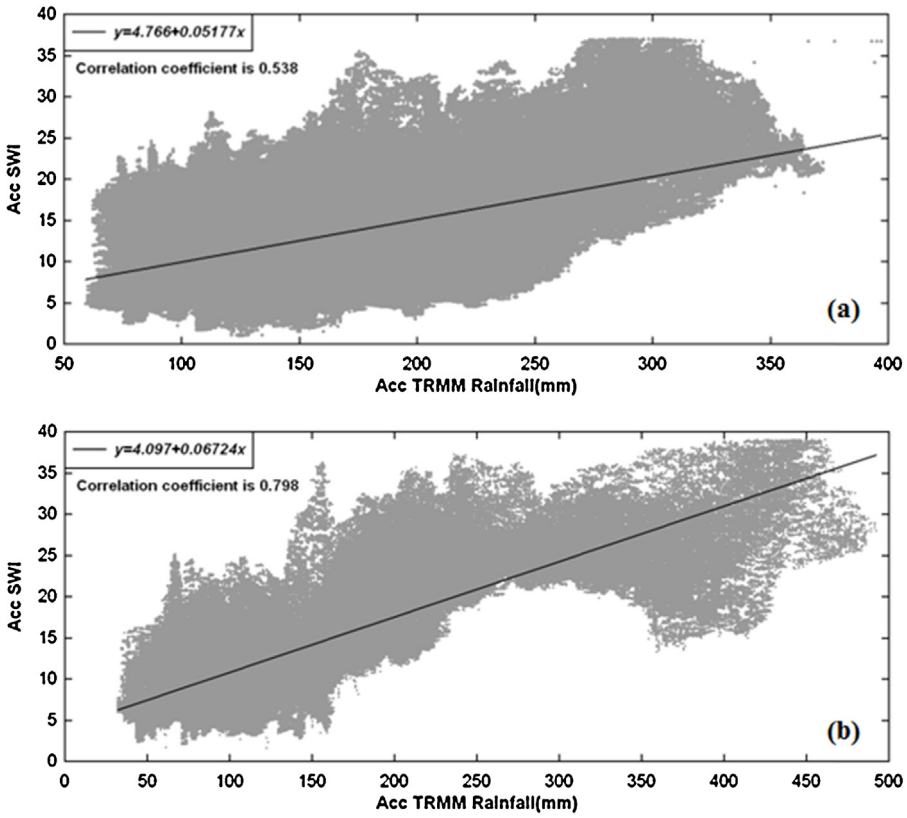

Fig. 8. (a) Comparison of cumulated rainfall and SWI in 2000–01. (b) Comparison of cumulated rainfall and SWI in 2004–05.

spatial pattern of SWDI in 2005: 17 and as indicated the areas with SWDI < 0 has been reduced to 50% in comparison to the same day in 2001. Also, the wet spell (SWDI > 0) is completely dominant in the western and southern areas and SWDI approaches 3 as shown by a few pixels. However, no significant difference was observed for the SWDI in the eastern parts compared to the same day in 2001.

In Fig. 4c and d, maps of SWDI in another time segment (DOY: 73) in the year 2001 and 2005 is compared. SWDI value in 2001: 73 (Fig. 4c) varies from −0.5 to 0 in 65% of the area, which indicates a slight increase in SWDI in comparison to the previous time segment in the same year (2001: 17). Comparing SWDI in two time sections in 2005, we can conclude that during 56 days the maximum SWDI has been decreased but the area with SWDI > 0 has increased.

In DOY 185 of both 2001 and 2005 (Fig. 4e and f) an inclination was observed in SWDI values. In 2001: 185, in spite of being in a dry period, drought spell was almost eliminated in the eastern regions. The western regions were still in a drought spell with deteriorating conditions (Fig. 4e). Transformation to the wet spell continues to the end of the dry period (DOY 209 of 2001) – meaning the end of dry spell in the area.

In same DOY in 2005 (Fig. 4f), the whole area transitioned toward a dry spell and quickly turns to a wet spell at the end of the wet period (DOY 209 of 2005). Altogether, in 184 days of the dry period (309 days from 2000: 273–2001: 209) SWDI < 0 was observed in more than 50% of the area.

The mean value variation of NDVI, SWI and LST for the two periods have been compared using the Duncan test (Tables 1 and 2) and shown in Figs. 5 and 6 in both irrigated and rain-fed farms from all over the area. For this purpose, each period (dry or wet) was defined as a treatment and each time period was considered a block. The results indicated that the differences between global means are significant (at 0.01 level of significance). This confirms that the amount of soil moisture, LST and NDVI in the period 2004–05 varies considerably from its values in the period of 2000–01 in both rain-fed and irrigated lands (Tables 2 and 3). The only exception was the NDVI values in the rain-fed farms didn't show a significant difference between the two periods.

To evaluate the newly developed SWDI drought Index in a smaller scale, the temporal variation of mean SWDI values in an irrigated farmland (Lat: 32°48′ Lon: 51°38′) were compared to a rain-fed farmland (Lat: 31°14′ Lon: 51°00′) that both have an area of 9 pixels (about 56 ha) in Fig. 7. Dry and wet spell dominance is quite evident in 2000–01 and 2004–05, respectively.

SWDI values vary from −1.7 to 1.2 in the rain-fed farmland but in the irrigated farmland it varies from −0.3 to 0.75. This difference could be caused by using water to overcome soil moisture deficit in the irrigated farmland during the dry period. On the other hand, this confirms that the SWDI responds well to the soil moister presence. Comparing the SWI and SWDI values (Figs. 5a, 6a and7), it appears that an increase in soil moisture does not in itself represent the end of a dry spell and the effect of its values in the previous months should be considered.

According to Fig. 7a and b, the maximum difference of SWDI mean value occurred within DOY 17–30 in both sample farms. These occurred almost simultaneously with the minimum values of NDVI and LST (Figs. 5 and 6) in all farm lands of the area (dormancy phase). It seems the lack of vegetation cover leads to an increase in intensity of both the wet spell in a wet period and the dry spell in a dry period. In other words, the existence of vegetation cover plays a moderating role in soil moisture variation.

SWDI values in sample farms also show a shift from dry spell to wet spell at the end of 2001 and vice versa at the end of 2005 (Fig. 7a and b). This has been seen and discussed before regarding Fig. 4. This supports the probability of change in drought condition at the end of both wet and dry periods in the area.

Finally, the correlation of cumulative SWI and cumulative rainfall at the end of both dry and wet periods was analyzed to see the validation of results derived from SWI (Fig. 8). As expected, the cumulative rainfall (calibrated TRMM data) and SWI were highly matched ($R^2 = 0.8$) which confirms the effect of rainfall on SWI. However, in the dry period, correlations reach to only 50 percent. This shows that in the dry period, radiation and temperature affect soil water contents more than rainfall.

4. Conclusions

In this study, a drought index (SWDI) was developed using SWI (derived from NDVI-LST triangular concept) to study the soil moisture variation in the wet and dry period using remotely satellite data with spatial resolution of 250 m every 8 days.

The results indicated that SWDI is capable of identifying and distinguishing dry and wet events both temporally and spatially. Accordingly, identifying a time interval as a wet or a dry period for a large region is not acceptable. A broad range of wet and dry events that occurred at one time in the area shows the inability to determine drought occurrence based on a limited number of weather reports.

Furthermore, comparing SWI with SWDI values showed that increases in moisture cannot indicate the end of a drought in itself and the effect of previous time steps should be considered. Results also showed that the presence of vegetation plays a modifying role in both wet and dry conditions.

References

Adegoke, J.O., Carleton, A.M., 2002. Relations between soil moisture and satellite vegetation indices in the U.S. corn belt. Journal of Hydrometeorology 3, 395–405.

Akbari, M., Toomanian, N., Droogers, P., Bastiaanssen, W., Gieske, A., 2007. Monitoring irrigation performance in Esfahan, Iran, using NOAA satellite imagery. Agricultural Water Management 88, 99–109.

Carlson, T., 2007. An overview of the "Triangle Method" for estimating surface evapotranspiration and soil moisture from satellite imagery. Sensors 7, 1612–1629.

Cheng, Y.B., Ustin, S.L., Riaño, D., Vanderbilt, V.C., 2008. Water content estimation from hyperspectral images and MODIS indexes in Southeastern Arizona. Remote Sensing of Environment 112, 363–374.

Crow, W.T., Kustas, W.P., Prueger, J.H., 2008. Monitoring root-zone soil moisture through the assimilation of a thermal remote sensing-based soil moisture proxy into a water balance model. Remote Sensing of Environment 112, 1268–1281.

De Ridder, K., 2000. Quantitative estimate of skin soil moisture with the special sensor microwave/imager. Boundary-Layer Meteorology 96, 421–432.

Gao, B.C., 1996. NDWI – a normalized difference water index for remote sensing of vegetation liquid water from space. Remote Sensing of Environment 58, 257–266.

Gillies, R.R., Carlson, T.N., 1995. Thermal remote sensing of surface soil water content with partial vegetation cover for incorporation into climate models. Journal of Applied Meteorology 34, 745–756.

Huete, A.R., Liu, H.Q., Batchily, K., van Leeuwen, W., 1997. A comparison of vegetation indices over a global set of TM images for EOS-MODIS. Remote Sensing of Environment 59, 440–451.

Keshavarz, M.R., Vazifedoust, M., Alizadeh, A., Asadi, A., 2011. Trend analysis of Soil Wetness Index derived from optical satellite data. In: International Conference of ISPRS (WGII/4,7).

Kogan, F., 1997. Global drought watch from space. Bulletin of the American Meterological Society 78 (4), 621–635.

Kuenzer, C., Bartalis, Z., Schmidt, M., Zhaoa, D., Wagner, W., 2008. TREND analyzes of a global soil moisture time series derived from ERS-1/-2 scatterometer data: floods, droughts and long term changes. The International Archives of the Photogrammetry, Remote Sensing and Spatial Information Sciences XXXVII (Part B7) (Beijing, China).

Mallick, K., Bhattacharya, B.K., Patel, N.K., 2009. Estimating volumetric surface moisture content for cropped soils using a Soil Wetness Index based on surface temperature and NDVI. Agricultural and Forest Meteorology 149, 1327–1342.

Marshall, G.S., 2005. Drought Detection and Quantification using Field-Based Spectral Measurements of Vegetation in Semi-Arid Regions. New Mexico Institute of Mining and Technology Department of Earth and Environmental Science, (M.Sc Thesis).

Mattia, F., Satalino, G., Pauwels, V.R.N., Loew, A., 2008. Soil moisture retrieval through a merging of multi-temporal L-band SAR data and hydrologic modeling. Hydrology and Earth System Sciences 5, 3479–3515.

Moran, M.S., Peters-Lidard, C.D., Watts, J.M., McElroy, S., 2004. Estimating soil moisture at the watershed scale with satellite-based radar and land surface models. Canadian Journal of Remote Sensing 30 (5), 805–826.

Narasimhan, B., Srinivasan, R., 2005. Development and evaluation of Soil Moisture Deficit Index (SMDI) and Evapotranspiration Deficit Index (ETDI) for agricultural drought monitoring. Agricultural and Forest Meteorology 133, 69–88.

Peñuelas, J., Piñol, J., Ogaya, R., Filella, I., 1997. Estimation of plant water concentration by the reflectance water index WI (R900/R970). International Journal of Remote Sensing 18, 2869–2875.

Peters, A.J., Rundquist, D.C., Wilhite, D.A., 1991. Satellite detection of the geographic core of the 1988 Nebraska drought. Agricultural and Forest Meteorology 57, 1–3.

Peters, E., 2003. Propagation of Drought through Groundwater Systems-Illustrated in the Pang (UK) and Upper-Guadiana (ES) Catchments. Wageningen University, The Netherlands (Ph.D. Thesis).

Palmer, W.C., 1965. Meteorological Drought. Research Paper No. 45. US Weather Bureau, Washington, DC.

Qui, H., 2006. Thermal Remote Sensing of Soil Moisture: Validation of Presumed Linear Relation between Surface Temperature Gradient and Soil Moisture Content. Project Report. Civil and Environmental Engineering department, The University of Melbourne.

Stisen, S., Sandholt, I., Nöörgard, A., Fensholt, R., Jensen, K.H., 2008. Combining the method with thermal inertia to estimate regional evapotranspiration-applied to MSG-SEVIRI data in the Senegal River basin. Remote Sensing of Environment 112, 1242–1255.

Ustin, S.L., Darling, D., Kefauver, S., Greenberg, J., Cheng, Y.B., Whiting, M.L., 2004. Remotely sensed estimates of crop water demand. Paper presented at S.P.I.E. In: The International Symposium on Optical Science and Technology. 49th Annual Meeting, 2–6 August, Denver, CO.

Verstraeten, W.W., 2006. Integration of Remotely Sensed Hydrological Data into an Ecosystem Carbon Flux Model. Katholieke University the Leuven (Ph.D. Thesis).

Wang, K.C., Li, Z.Q., Cribb, M.M., 2006. Estimation of evaporative fraction from a combination of day and night land surface temperatures and NDVI: a new method to determine Priestley–Taylor parameter. Remote Sensing of Environment 102, 293–305.

Wang, X., Xie, H., Guan, H., Zhou, X., 2007. Different responses of MODIS-derived NDVI to root-zone soil moisture in semi-arid and humid regions. Journal of Hydrology 340, 12–24.